Supporting Information

Nitrogen doped porous carbon fiber/vertical graphene as efficient polysulfide conversion catalyst for high performance lithium sulfur batteries

Junsheng Lin[a], Yangcheng Mo[a], Shiwen Li[a], Jie Yu[a*]

[a]Shenzhen Engineering Lab for Supercapacitor Materials, Shenzhen Key Laboratory for Advanced Materials, School of Material Science and Engineering, Harbin Institute of Technology, Shenzhen, University Town, Shenzhen 518055, China

[*] Corresponding author: E-mail address: jyu@hit.edu.cn (J. Yu).

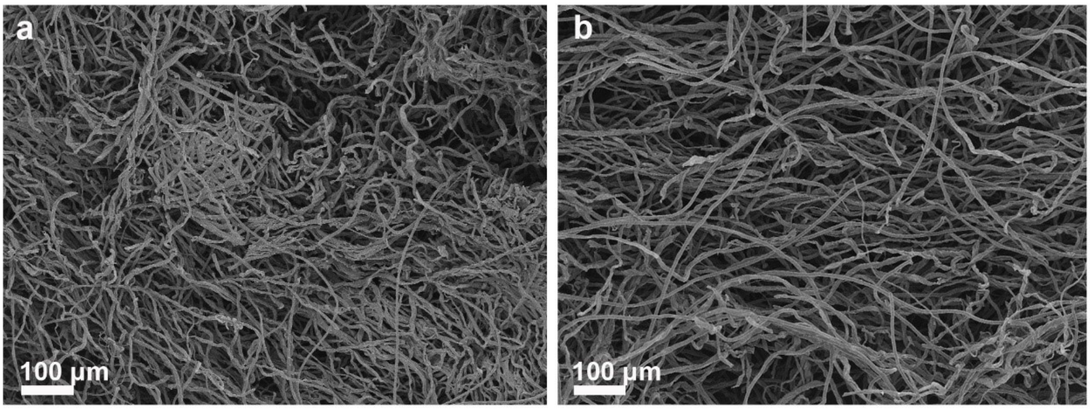

Fig. S1 SEM images of cotton pad.

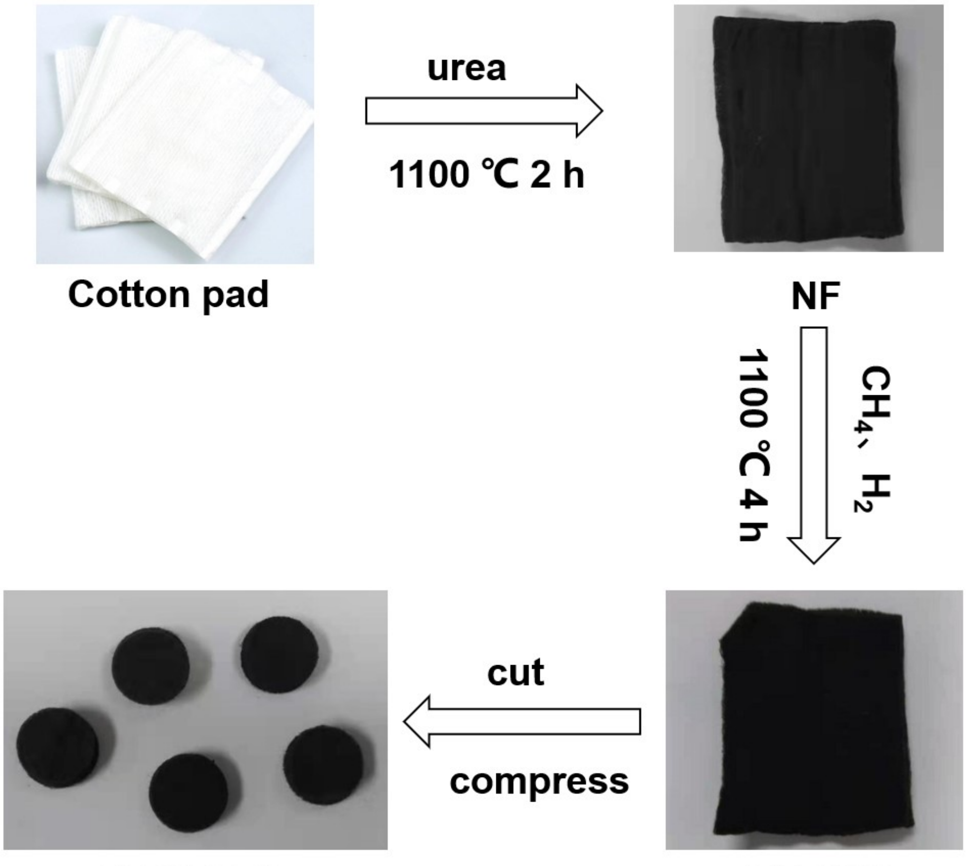

Fig. S2 Digital images of different samples.

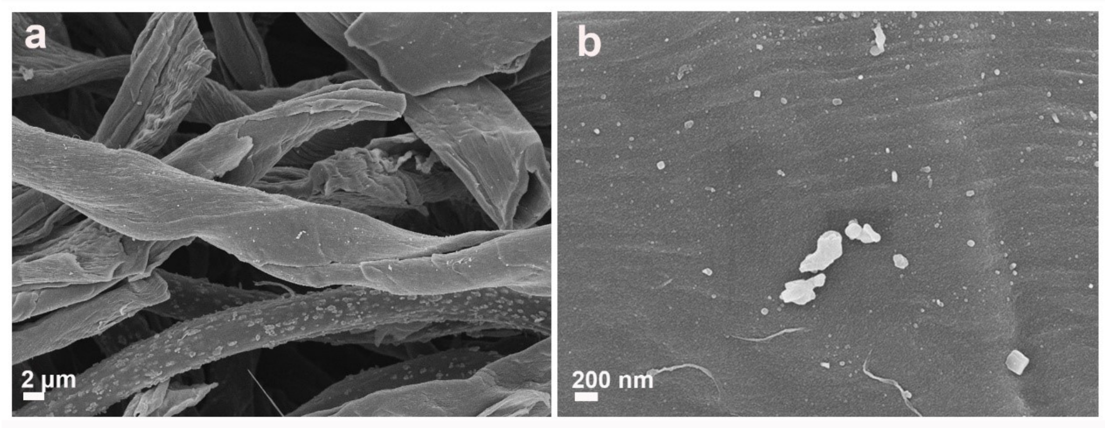

Fig. S3 SEM images of CF.

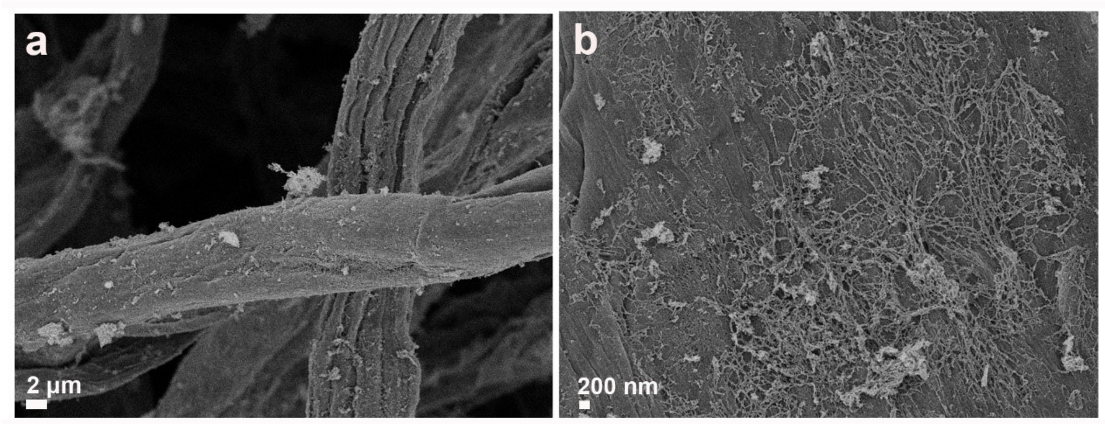

Fig. S4 SEM images of NF.

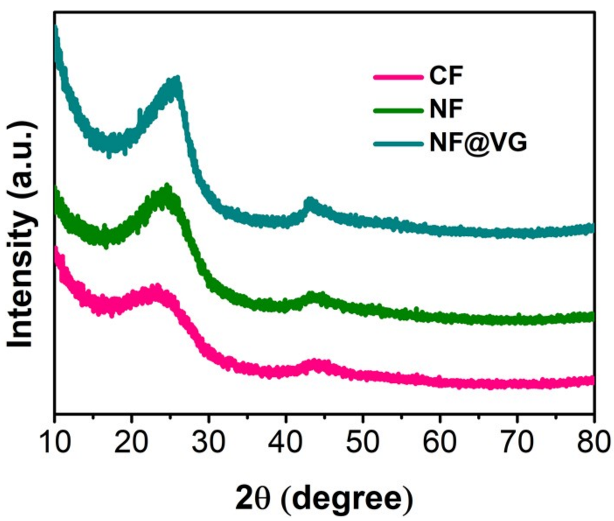

Fig. S5 XRD patterns of CF, NF and NF@VG.

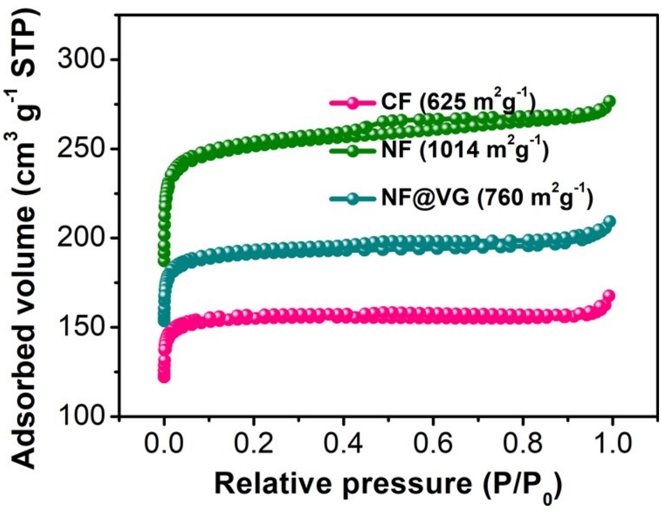

Fig. S6 N_2 adsorption and desorption isotherms of CF, NF and NF@VG.

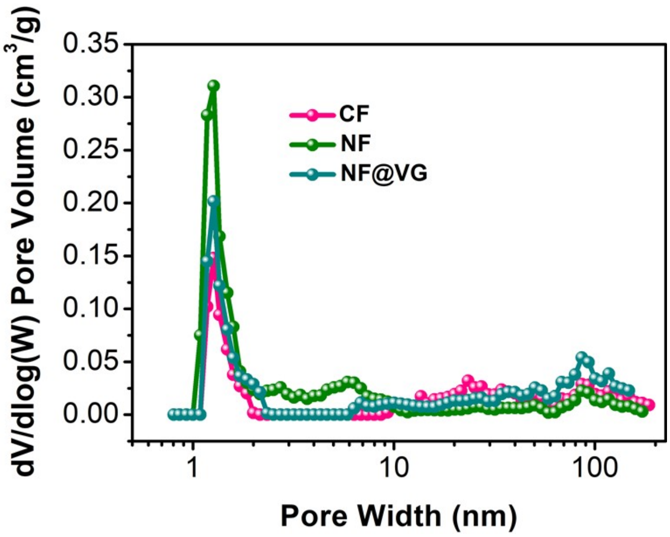

Fig. S7 Pore size distribution of CF, NF and NF@VG.

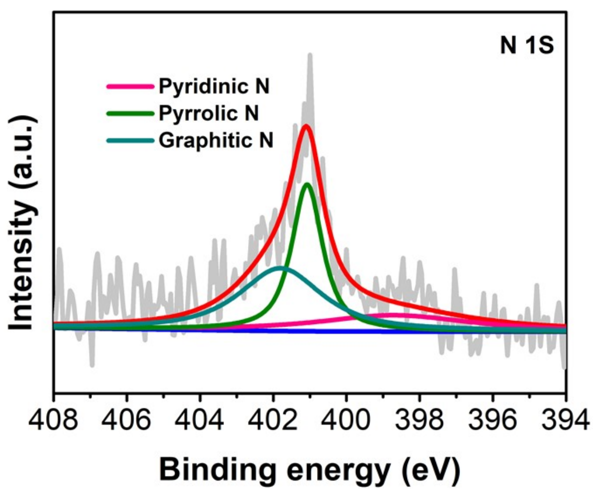

Fig. S8 N 1s spectrum of NF.

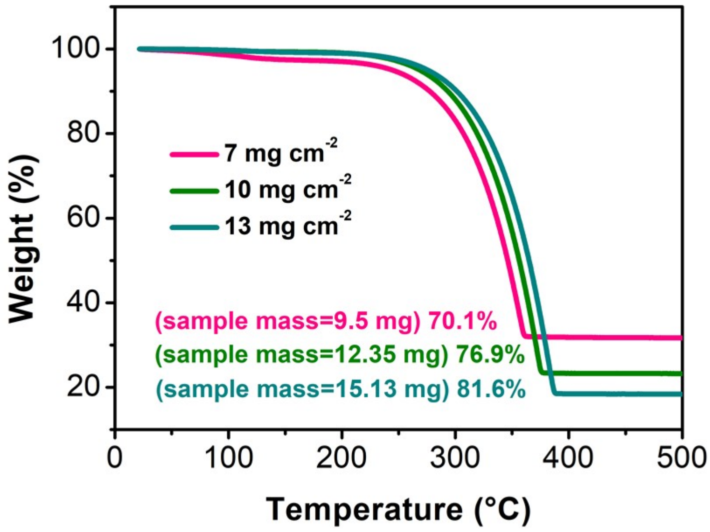

Fig. S9 TGA curves of NF@VG-S.

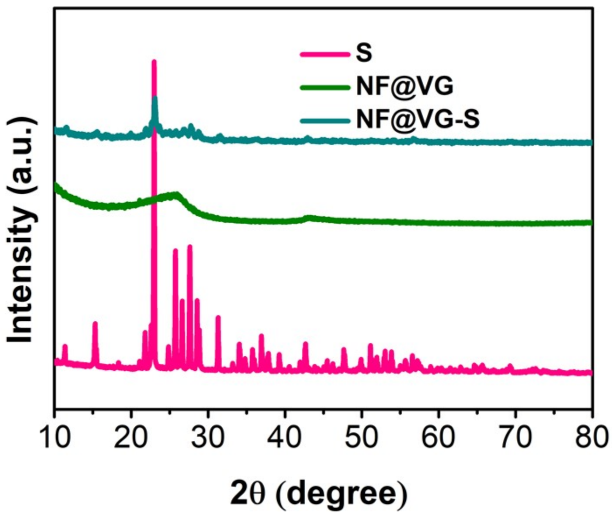

Fig. S10 XRD patterns of S, NF@VG and NF@VG-S.

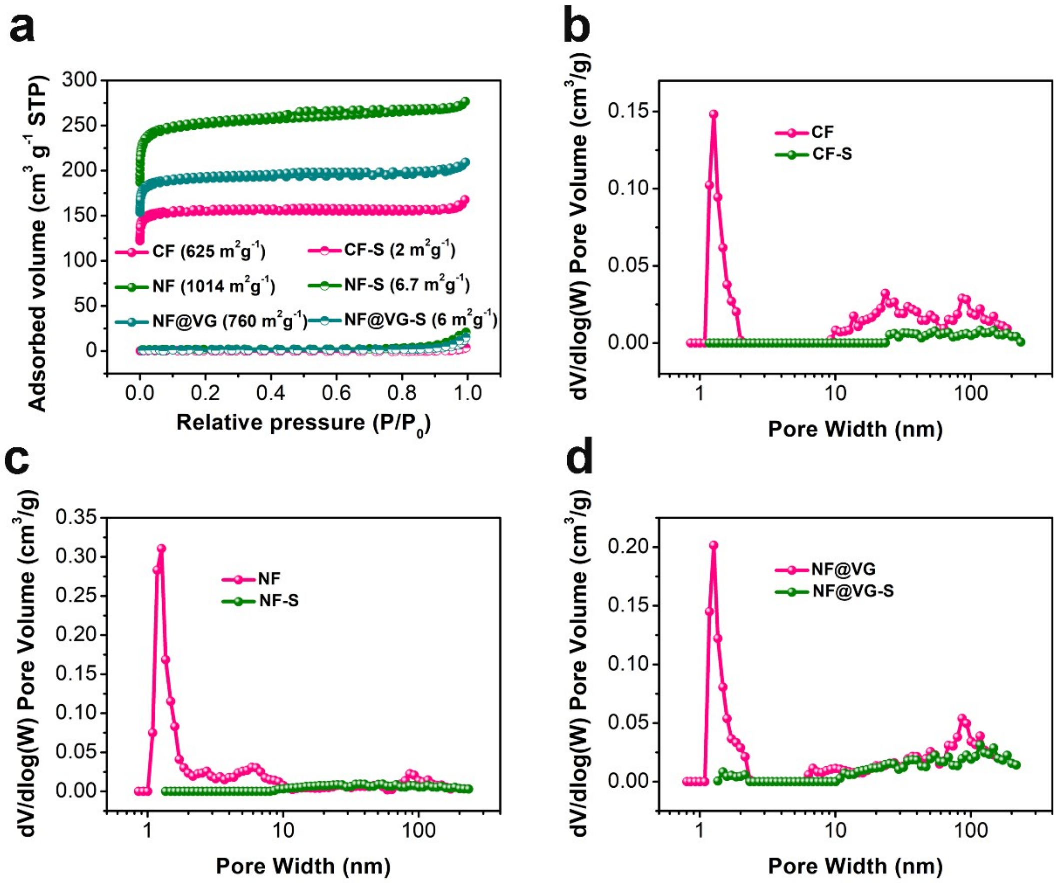

Fig. S11 N_2 adsorption and desorption isotherms (a) of CF, CF-S, NF, NF-S, NF@VG and NF@VG-S, pore size distribution (b-d) of CF and CF-S (b), NF and NF-S (c), NF@VG and NF@VG-S (d).

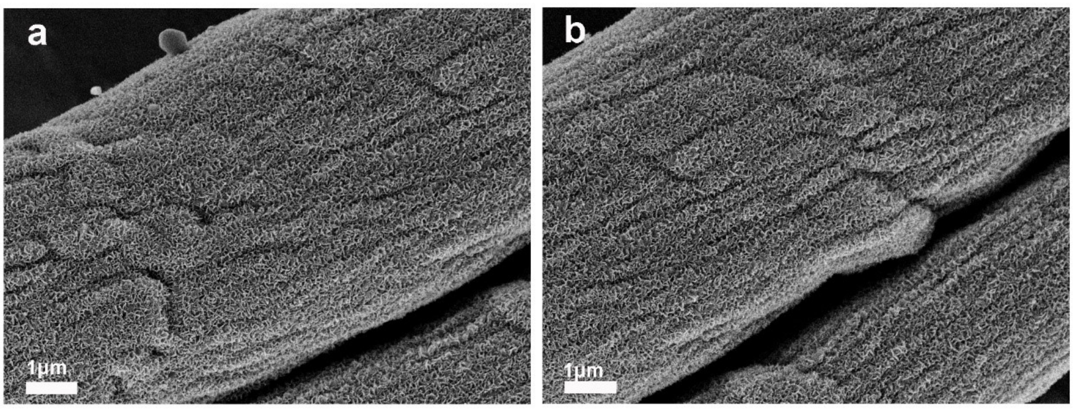

Fig. S12 SEM images of NF@VG-S.

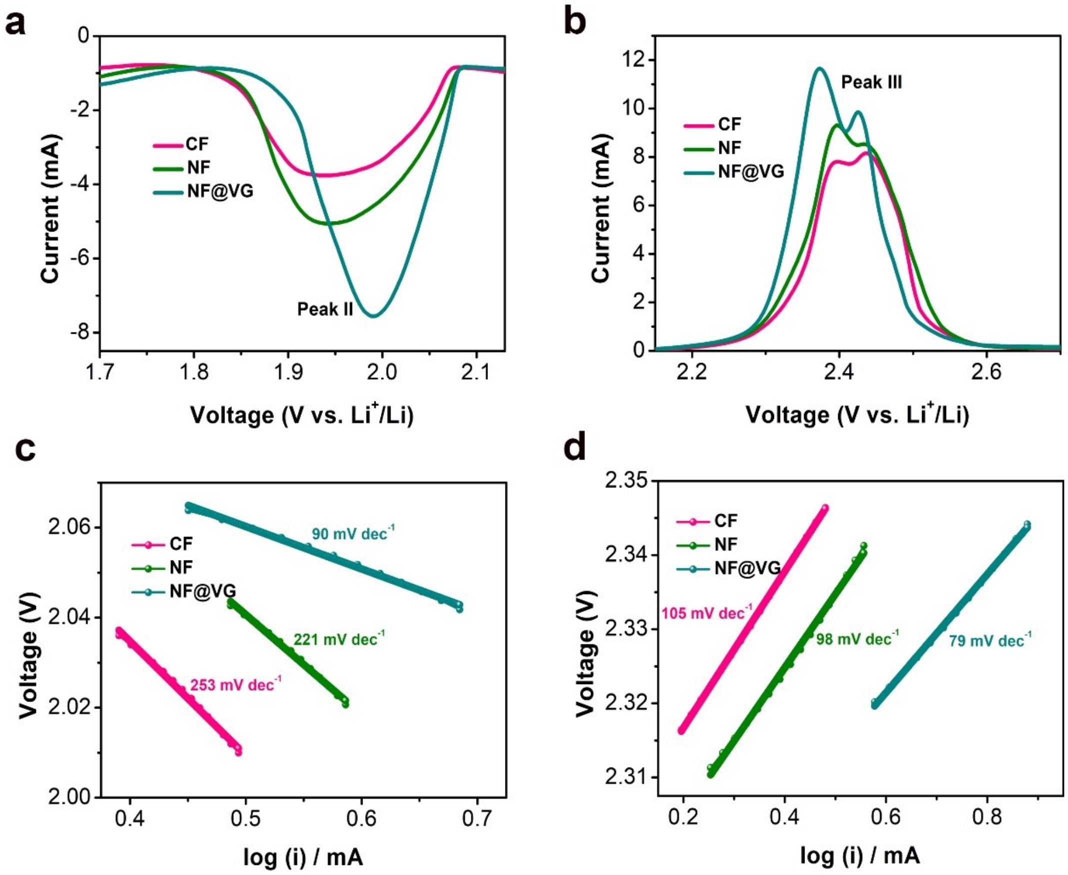

Fig. S13 CV profiles of an enlarged view in (a) peak II and (b) peak III of Li-S batteries with different cathodes. (c, d) Tafel plots calculated from reduction peak II and oxidation peak III.

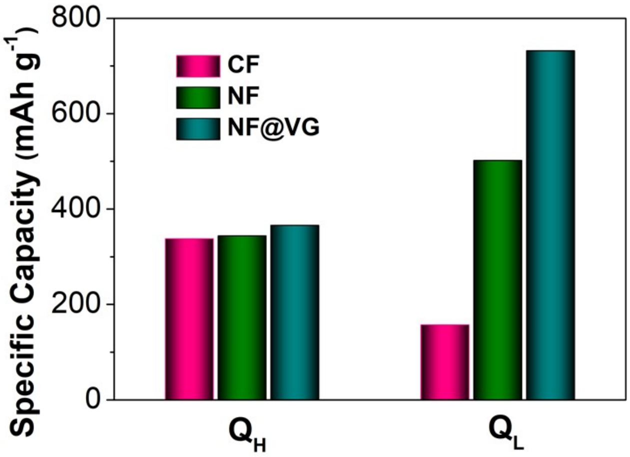

Fig. S14 The comparison of the discharge capacities for upper-platform discharge capacity (Q_H) and lower-platform discharge capacity (Q_L).

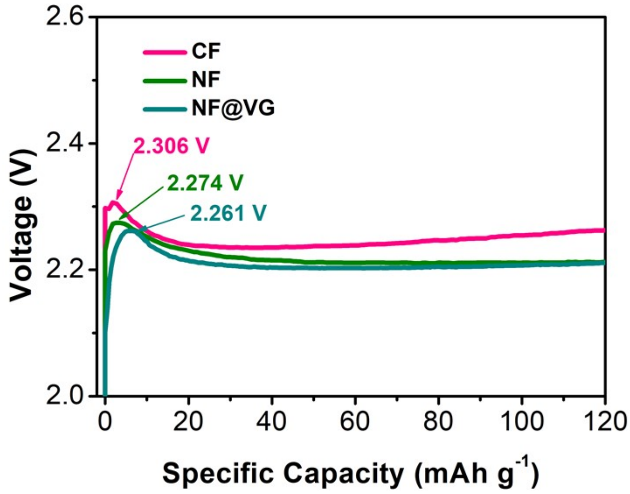

Fig. S15 Charge curves comparison of the CF-S, NF-S and NF@VG-S cathodes at 0.2 C

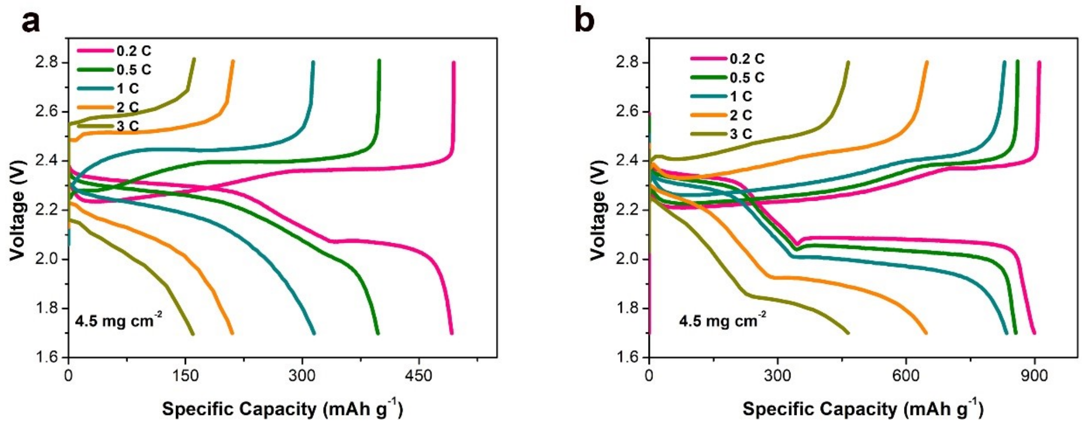

Fig. S16 Galvanostatic discharge-charge curves of the CF-S (a) and NF-S (b) cathodes at different rates.

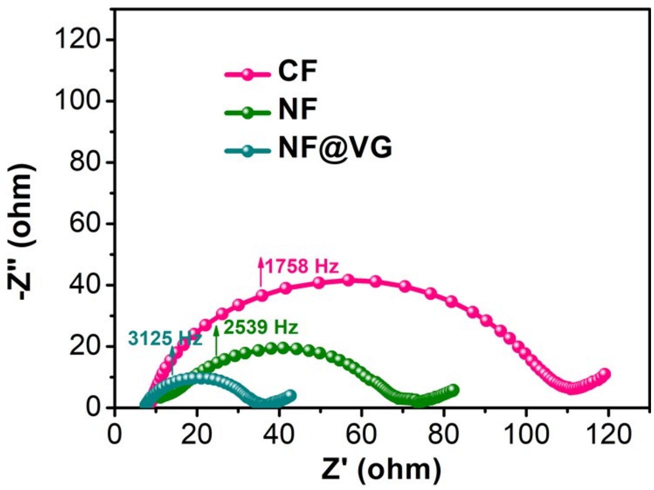

Fig. S17 Electrochemical impedance spectras of CF-S, NF-S and NF@VG-S cathodes before cycling.

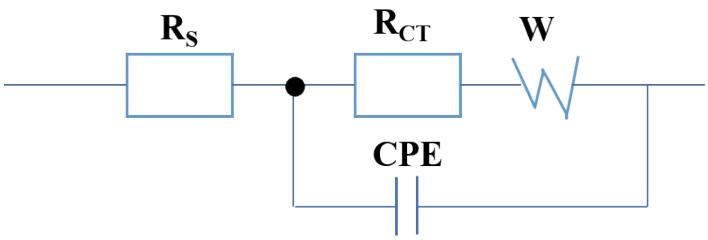

Fig. S18 Equivalent circuit for fitting the electrochemical impedance spectra of the batteries. Rs is the bulk resistance of the batteries. and Rct is the resistance of charge transfer. CPE is a constant phase angle element corresponding to the double-layer capacitance, W is the Warburg impedance related to ion diffusion.

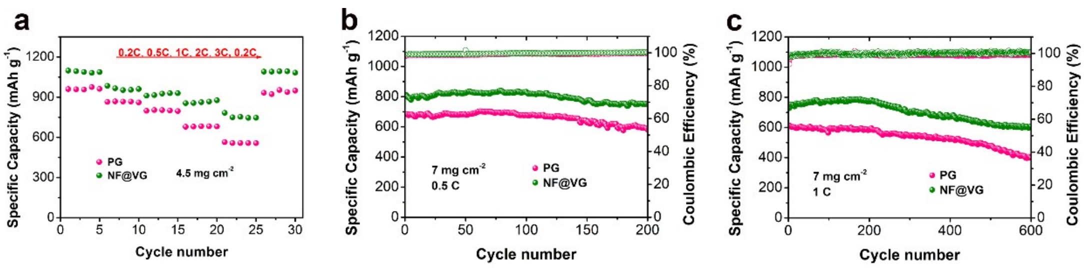

Fig. S19 (a-c) Rate performance (a). Cycle performance at 0.5 C (b). Long-term cycling performance at 1 C (c) of PG-S and NF@VG-S cathodes.

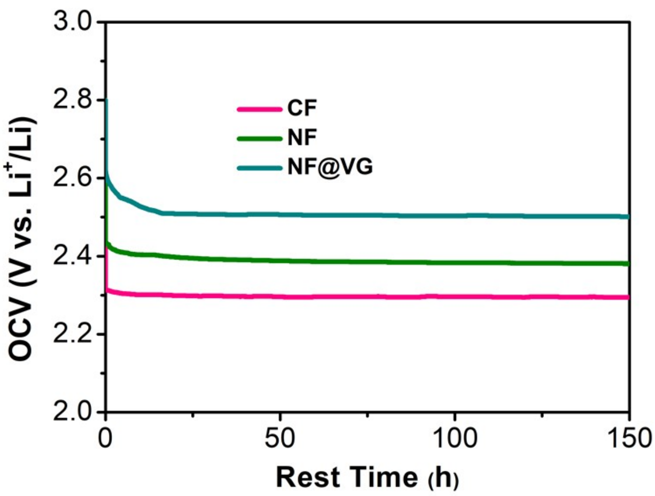

Fig. S20 Self-discharge behavior of the batteries with CF-S, NF-S and NF@VG-S cathodes

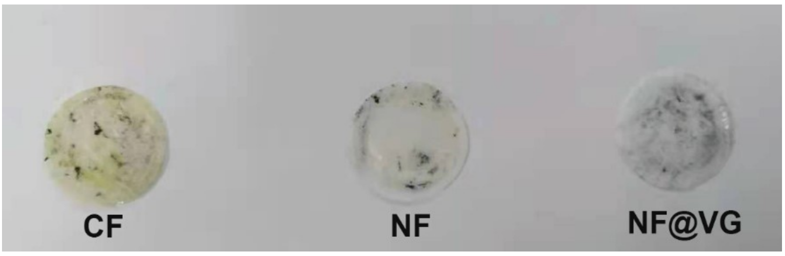

Fig. S21 Photographs for PP separators of batteries with (a) CF-S, (b) NF-S and (c) NF@VG-S cathodes toward Li metal anode after 200 cycles at 0.5 C

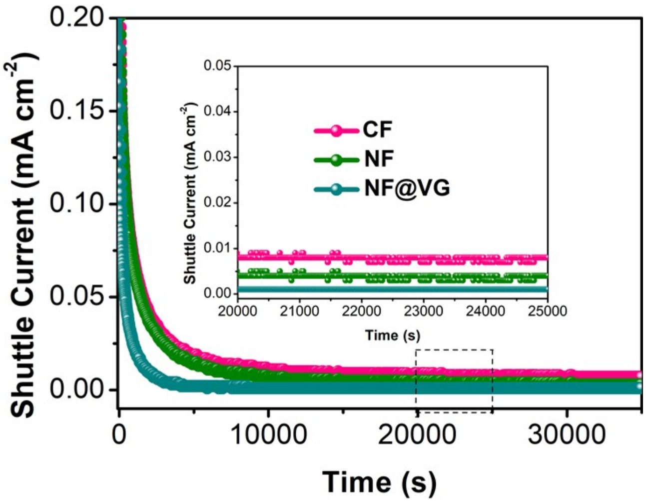

Fig. S22 the shuttle current test of the batteries with CF-S, NF-S and NF@VG-S cathodes

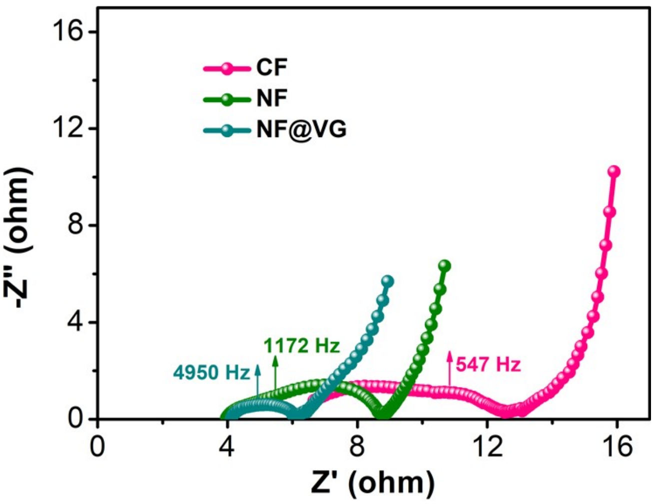

Fig. S23 Electrochemical impedance spectras of symmetric batteries with CF, NF and NF@VG electrodes

Table S1 Comparison of areal capacities of NF@VG-S cathode with those of the recent publications in Li-S batteries with high sulfur loading of more than 4.5 mg cm^{-2}.

materials	Sulfur loading (mg cm^{-2})	Sulfur Content (%)	Electr-olyte/ sulfur ratio (E/S)	Rate (C)	Cycle number	Areal capacity (mAh cm^{-2})	Final capacity (mAh cm^{-2})	Ref.
Co@NHC MSs	5.1	72.4	10	0.1	50	5	4	1
3DMPGF	13	90	-	0.1	50	10.3	5.9	2
NC/G	5.6	72	8	0.1	50	6.2	4	3
NOGB	4.4	53	12	0.1	50	6	3.3	4
Fe_3C-MC	9	80	6	0.1	100	8.77	6.29	5
CF@CNT s/MgO	14.4	78	6.9	0.1	50	10.4	8.8	6
$Fe_{3x}C$@ C-500	7	60	-	0.1	50	5.6	5	7
Fe_3C/NC	5	65	10	0.1	100	4.9	3.6	8
NF@VG	**13**	**81.6**	**4.8**	**0.1**	**100**	**12.8**	**11.2**	**This work**

References

1. L. Su, J. Zhang, Y. Chen, W. Yang, J. Wang, Z. Ma, G. Shao and G. Wang, *Nano Energy*, 2021, **85**, 105981.
2. L. Lu, J. T. M. De Hosson and Y. Pei, *Carbon*, 2019, **144**, 713-723.
3. H. Xu, Q. Jiang, B. Zhang, C. Chen and Z. Lin, *Adv. Mater.*, 2020, **32**, e1906357.
4. M. Shi, S. Zhang, Y. Jiang, Z. Jiang, L. Zhang, J. Chang, T. Wei and Z. Fan, *Nano-micro Lett.*, 2020, **12**, 146.

5. H. Li, S. Ma, H. Cai, H. Zhou, Z. Huang, Z. Hou, J. Wu, W. Yang, H. Yi, C. Fu and Y. Kuang, *Energy Storage Mater.*, 2019, **18**, 338-348.
6. M. Xiang, H. Wu, H. Liu, J. Huang, Y. Zheng, L. Yang, P. Jing, Y. Zhang, S. Dou and H. Liu, *Adv. Funct. Mater.*, 2017, **27**, 1702573.
7. Y. Zhang, G. Li, J. Wang, G. Cui, X. Wei, L. Shui, K. Kempa, G. Zhou, X. Wang and Z. Chen, *Adv. Funct. Mater.*, 2020, **30**, 2001165.
8. C. Zhou, X. Li, H. Jiang, Y. Ding, G. He, J. Guo, Z. Chu and G. Yu, *Adv. Funct. Mater.*, 2021, **31**, 2011249.